Optical Materials 174 (2026) 117999

Contents lists available at ScienceDirect

Optical Materials

journal homepage: www.elsevier.com/locate/optmat

Short Communication

Confusion between Raman spectrum and luminescence: a case study of Eu^{3+} in $Cs_2NaEuCl_6$

Peter A. Tanner

Department of Applied Biology and Chemical Technology, The Hong Kong Polytechnic University, Hung Hom, Kowloon, Hong Kong Special Administrative Region of China

ARTICLE INFO

Keywords:
Raman
Luminescence
Lanthanide ion
Elpasolite
Halide double perovskite

ABSTRACT

Some lanthanide ions have electronic energy levels extending from the far infrared to the vacuum ultraviolet. Without cross-relaxation between levels and other nonradiative depopulation mechanisms, and with adequate spacing between the energy levels, luminescence can be observed. When recording a Raman spectrum of a lanthanide compound, care should be taken to select an appropriate wavelength to avoid luminescence. Two recent examples illustrate results when this is not followed.

We previously commented upon the appearance of additional bands in the Raman spectrum of a Nd^{3+} compound [1]. These bands were 'hot' luminescence transitions so that upon cooling the sample they disappeared. Since many lanthanide ions have energy levels spanning from the far infrared to the vacuum ultraviolet spectral regions [2] one must be cautious in choosing an appropriate laser wavelength for recording a Raman spectrum in order to avoid luminescence. Recently, we have observed two studies of another lanthanide ion, Eu^{3+} in $Cs_2NaEuCl_6$, and we comment upon these [3,4]. The vibrational and electronic spectra of this compound were reported many decades ago [5–16].

It is not appropriate [4] to describe the peaks in the emission spectra of $Cs_2NaEuCl_6$ as electric dipole (ED) transitions which split into multiple components due to crystal field effects, as we now explain. In fact, the Eu^{3+} ion is located with octahedral chloride coordination at a site of O_h symmetry in this compound [17] and the emission spectra have been interpreted and fitted [8,18]. The $4f^6 - 4f^6$ transitions of this ion are ED forbidden and forced ED forbidden to first order. The relevant energy levels of Eu^{3+} are shown in Fig. 1(a). Part of the visible emission spectra at room temperature (black spectrum, Fig. 1(b)), comprise a strong $^5D_0 \rightarrow {}^7F_1$ transition (line D), orbitally allowed by the magnetic dipole (MD) mechanism, together, at longer wavelength, with one-phonon odd-parity vibrational sidebands (A, B, C) based upon unobserved electronic origins. The multiple components A, B, C described in Ref. [4] comprise different and unresolved vibronic origins. At lower temperature, fine structure is resolved (red spectrum, Fig. 1(b)) and the vibronic assignments have previously been given and are not repeated here [8,14]. At room temperature, anti-Stokes vibronic bands (A) are observed. In particular, to higher energy in the green spectral region, weak emission is also observed from the $^5D_1$ level (Fig. 1(a)). It is relatively stronger at low temperature and has been reported and assigned [6–8].

Rao et al. [3] and Bouzidi et al. [4] recently reported the Raman spectrum of $Cs_2NaEuCl_6$. The XPS spectrum in Ref. [3] and the electronic absorption spectrum in Ref. [4] indicate the presence of Eu^{2+} in the samples. The Raman spectrum differs from earlier reports since the vibrational energies are not the same [7,12,13] and are not typical of hexachloroelpasolites. The Fourier-transform infrared absorption spectra of lanthanide elpasolites have previously been reported [19]. The vibrational energies have been fitted according to the GF matrix method [7,11] and the experimental values for the internal normal modes are given in Table 1. In addition to these vibrations there are external modes according to the unit cell group analysis [15], with experimentally determined wavenumbers: S_3, the t_{1g} $LnCl_6$ rotatory mode ~20 cm^{-1}; S_5, the Cs t_{2g} translatory mode 46 cm^{-1}; S_8, the t_{1u} Na–Cl stretch, 166 cm^{-1} and S_9, the t_{1u} Cs translatory mode, 55 cm^{-1}. Hence, the Raman spectrum, comprising active gerade modes, is expected to show the internal ν_1 a_{1g} 290 cm^{-1}, ν_2 e_g 228 cm^{-1}, ν_5 t_{2g} 118 cm^{-1} modes and the external t_{2g} 46 cm^{-1} vibration.

The wavenumbers of Raman modes reported in Refs. [3,4] are included in Table 2 with the assignments made by these authors in column 3. Our Raman spectrum between 30 and 750 cm^{-1} was recorded using 514.5 nm radiation at 120 K [7]. We previously noted [7] that the use of 457.9 nm radiation, and of 514.5 nm radiation outside this range, gave Eu^{3+} emission spectra. The laser wavelength given in Refs. [3,4] is 532 nm. This corresponds to a frequency-doubled YAG:Nd laser

E-mail addresses: peter.a.tanner@gmail.com, monkey.tanner@polyu.edu.hk.

https://doi.org/10.1016/j.optmat.2026.117999
Received 15 December 2025; Received in revised form 14 February 2026; Accepted 28 February 2026
Available online 1 March 2026

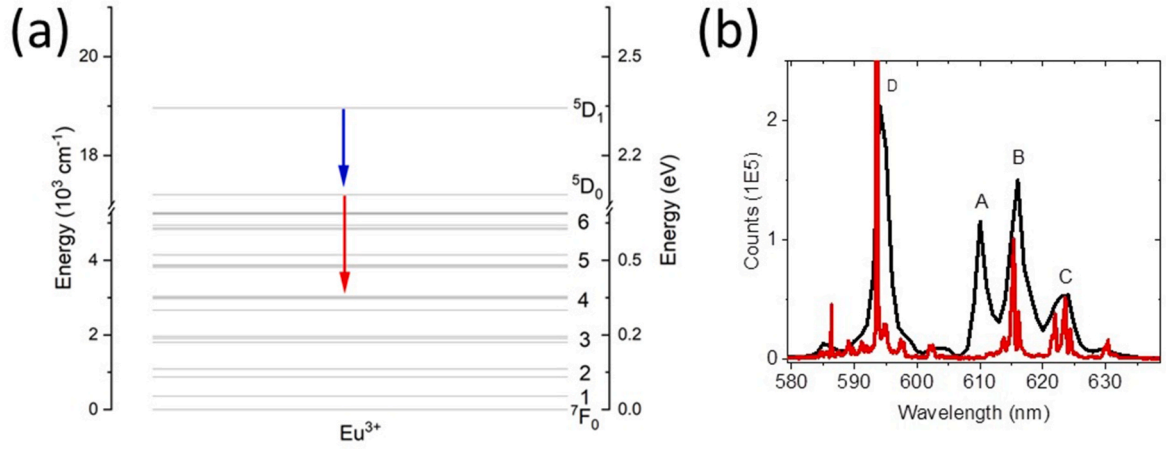

Fig. 1. (a) Relevant energy levels of Eu^{3+} in $Cs_2NaEuCl_6$. At room temperature, visible luminescence is observed from $^5D_0$ Γ_1 (17207 cm^{-1}) and with weak intensity from $^5D_1$ Γ_4 (18959 cm^{-1}) [7]. (b) Comparison of 10 K (red) and room temperature (black) 463 nm excited emission spectra of $Cs_2NaEuCl_6$ (the relative intensities are not to scale). (For interpretation of the references to colour in this figure legend, the reader is referred to the Web version of this article.)

Table 1
Observed vibrational wavenumbers (cm^{-1}) of internal modes in $Cs_2NaEuCl_6$ [7]. The energies of ungerade modes are taken from vibronic spectra and are averaged over transverse and longitudinal components where applicable.

Mode	ν_1	ν_2	ν_3	ν_4	ν_5	ν_6
Symmetry (O_h)	a_{1g}	e_g	t_{1u}	t_{1u}	t_{2g}	t_{2u}
Wavenumber	290	228	260	105	118	79

Table 2
Reassignment of the bands in Figure 1e of Ref. [3] and Figure 5 of Ref. [4].

Reported Raman shift (cm^{-1}) [3]	Reported Raman shift (cm^{-1}) [4]	Assignment [3]	Approximate energy (cm^{-1})	Assignment and symmetry representation in O_h
66	67	t_{2g}	18723	$^5D_1T_{1g} \rightarrow {}^7F_0A_{1g}$ + ν_3 t_{1u} $^5D_1T_{1g} \rightarrow {}^7F_1T_{1g}$ - ν_4 t_{1u}
99	100	t_{2g}	18690	$^5D_1T_{1g} \rightarrow {}^7F_1T_{1g}$ - ν_6 t_{2u}
172	172	e_g	18617	$^5D_1T_{1g} \rightarrow {}^7F_1T_{1g}$
254	255	a_{1g}	18535	$^5D_1T_{1g} \rightarrow {}^7F_1T_{1g}$ + ν_6 t_{2u}, ν_4 t_{1u}
414	413	$2a_{1g}$	18375	$^5D_1T_{1g} \rightarrow {}^7F_1T_{1g}$ + ν_3 TO t_{1u}

operating at 1064.45 ± 0.03 nm. Hence the energy is 18789 cm^{-1}. The excitation is then into the $^7F_0A_{1g} \rightarrow {}^5D_1T_{1g} + S_8$ t_{1u} vibronic band, where the labels correspond to irreducible representations of the O_h point group. Our analysis is therefore based upon the thermal population of the one $^5D_1$ T_{1g} level.

The determined energies of peaks on a cm^{-1} scale are listed in column 4 of Table 2. In the next column 5 we have reassigned these bands according to emission from the $^5D_1$ T_{1g} level. Our previous assignment of the $^5D_1$ $T_{1g} \rightarrow {}^7F_0$ A_{1g} transition was at 18959 cm^{-1} at 120 K and 18968 cm^{-1} at room temperature [7] so that the terminal electronic state in Table 2 is $^7F_1$ T_{1g}, at ~360 cm^{-1} to lower energy of $^7F_0$. The value in column 4 of Table 2 differs by 9 cm^{-1} from this value, attributed to differences between air and vacuum wavenumbers, measurement temperature, experimental resolution and/or calibration errors.

In Table 2, according to the assignments in column 5, the zero-phonon line $^5D_1T_{1g} \rightarrow {}^7F_1T_{1g}$ is observed at 18617 cm^{-1}. Stokes and anti-Stokes bands are observed for this transition. Only one Stokes band is observed at 82 cm^{-1}. The band is so broad that the 105 cm^{-1} component merges into it. However, the anti-Stokes bands are observed for both the t_{1u} and t_{2u} bending modes. The calculated intensity ratio of these Stokes and anti-Stokes bands at room temperature, using the average frequency (79/105) of 92 cm^{-1} is 0.64. Consistent with this, the measurement of integrated areas in the brown and blue spectra of Fig. 5 in Ref. [4] gives the Stokes: anti-Stokes ratio of 0.59 ± 0.01. The assignment of the "414 cm^{-1} band" in Ref. [3] is incorrect and it clearly corresponds to the ν_3 vibronic origin of the $^5D_1T_{1g} \rightarrow {}^7F_1T_{1g} + \nu_3$ transition.

In summary, one must be cautious when recording the Raman spectra of luminescent materials and choose an exciting wavelength that does not lead to emission. It is advisable to employ different excitation wavelengths for comparison and to investigate the effect of cooling upon the spectrum of the sample. In the present case the latter choice would be appropriate to remove luminescence, or to use near 785 nm diode laser near infrared excitation. However, in the case of lanthanide ions with energy levels that can be excited by near infrared radiation an alternative choice of excitation wavelength may be required.

Declaration of competing interest

The authors declare that they have no known competing financial interests or personal relationships that could have appeared to influence the work reported in this paper.

Acknowledgements

Prof. Guohua Jia and Mr. Daiwen Xiao are thanked for recording the 10 K and room temperature spectra of $Cs_2NaEuCl_6$ in Fig. 1(b), respectively.

Data availability

Data will be made available on request.

References

[1] P.A. Tanner, C.S.K. Mak, G.G. Siu, Additional bands in the FT-Raman spectra of lanthanide compounds, Appl. Spectrosc. 56 (2002) 670–673.
[2] R.T. Wegh, A. Meijerink, R.-J. Lamminmäki, J. Hölsä, Extending Dieke's diagram, J. Lumin. 87–89 (2000) 1002–1004.
[3] Z. Rao, X. Zhao, X. Gong, Modeling of a single-band-ratiometric sensor based on lattice positive thermal expansion in Eu^{3+}-activated halide perovskite $Cs_2NaEuCl_6$, Small 20 (2024) 2406348.
[4] M. Bouzidi, A.A. Alatawi, A. Jebnouni, A.S. Aljaloud, M.A.F. Alshammari, A. A. AlDheirib, M.B. Bechir, M.K. Shakfa, Dual photonic–electronic behavior in

$Cs_2NaEuCl_6$ double perovskite: photoluminescence, photoconductivity, and structural stability for optoelectronic applications, Opt. Mater. 168 (2025) 117535.
[5] R.W. Schwartz, The electronic structure of $Cs_2NaEuCl_6$, Molec. Phys. 30 (1975) 81–95.
[6] O.A. Serra, L.C. Thompson, Emission spectra of $Cs_2NaEuCl_6$ and $Cs_2Na(Eu,Y)Cl_6$, Inorg. Chem. 15 (1976) 504–507.
[7] P.A. Tanner, Y.L. Liu, Raman, electronic raman and luminescence spectrum of $Cs_2NaEuCl_6$, J. Alloys Compd. 204 (1994) 207–214.
[8] J.P. Morley, T.R. Faulkner, F.S. Richardson, Optical emission spectra and crystal field analysis of Eu^{3+} in the cubic Cs_2NaYCl_6 host, J. Chem. Phys. 77 (1982) 1710–1733.
[9] M. Bettinelli, C.D. Flint, Energy migration and transfer in the $^5D_0$ state of $Cs_2NaEuCl_6$, J. Phys. Condens. Matter 3 (1991) 7053–7059.
[10] J.R.G. Thorne, M. Jones, C.S. McCaw, K.M. Murdoch, R.G. Denning, N. M. Khaidukov, Two-photon spectroscopy of europium(III) elpasolites, J. Phys. Condens. Matter 11 (1999) 7851–7866.
[11] P.A. Tanner, M.-Y. Shen, Superparametrization of low-temperature vibrational data for lanthanide hexahalides, Spectrochim. Acta 50 (1994) 997–1003.
[12] H.-D. Amberger, G.G. Rosenbauer, R.D. Fischer, The electronic structure of highly symmetrical compounds of the lanthanides and actinides-VII. The electronic raman spectra of the lanthanide elpasolites of the type $Cs_2NaLn(III)Cl_6$, J. Phys. Chem. Solid. 38 (1977) 379–385.
[13] H.-D. Amberger, R.D. Fischer, G.G. Rosenbauer, Zur elektronenstruktur hochsymmetrischer komplexe der lanthanoiden und actinoiden: IV. Das elektronische Raman-spektrum von $Cs_2NaEu(III)Cl_6$, Z. Phys. Chem. 102 (1976) 279–282.
[14] C.D. Flint, F.L. Stewart-Darling, Vibronic transitions in the luminescence spectrum of $Cs_2NaEuCl_6$, Molec. Phys. 44 (1981) 61–68.
[15] L. Ning, P.A. Tanner, S. Xia, Unit cell group analysis of rare earth elpasolites, Vib. Spectrosc. 31 (2003) 51–61.
[16] M. Bettinelli, C.D. Flint, $^7F_0 - {}^5D_0$ excitation spectrum of $Cs_2NaEuCl_6$ and $Cs_2NaY_{1-x}Eu_xCl_6$, Chem. Phys. Lett. 167 (1990) 45–48.
[17] G. Meyer, The synthesis and structures of complex rare-earth halides, Prog. Solid State Chem. 14 (1982) 141–219.
[18] P.A. Tanner, Spectra, energy levels and energy transfer in high symmetry lanthanide compounds, Top. Curr. Chem. 241 (2004) 167–278.
[19] A. Barbanel, G.P. Chudnovskaya, I. Gavrish, R.B. Dushin, V.V. Kolin, V.P. Kotlin, Spectral-luminescent properties of actinides in elpasolite structure, J. Radioanal. Nucl. Chem. 143 (1990) 113–123.